A new accelerated salt weathering test by RILEM TC 271-ASC

preliminary round robin validation

Lubelli, B.; Aguilar, A. M.; Beck, K.; De Kock, T.; Desarnaud, J.; Franzoni, E.; Gulotta, D.; Ioannou, I.; Kamat, A.; Menendez, B.

Check for updates

A new accelerated salt weathering test by RILEM TC 271-ASC: preliminary round robin validation

B. Lubelli ⓘ · **A. M. Aguilar** · **K. Beck** · **T. De Kock** · **J. Desarnaud** ·
E. Franzoni · **D. Gulotta** · **I. Ioannou** · **A. Kamat** · **B. Menendez** ·
I. Rörig-Dalgaard · **E. Sassoni**

Abstract Salt crystallization is a major cause of damage in porous building materials. Accelerated salt weathering tests carried out in the laboratory are among the most common methods to assess the durability of material to salt decay. However, existing standards and recommendations for salt weathering tests have limitations in terms of effectiveness and/or reliability. In the framework of the RILEM Technical Committee 271-ASC, a procedure has been developed which proposes a new approach to salt crystallization tests. It starts from the consideration that salt damage can be seen as a process developing in two phases: accumulation of the salt in the material and propagation of the decay. In the first phase, salts are introduced in the material and accumulate close to the evaporation surface, while in the second phase damage propagates because of repeated dissolution and crystallization cycles, induced by re-wetting with liquid water and by relative humidity changes. In this paper, the procedure is described and the results of a first round robin validation of the test, carried out on 7 materials and involving 10 laboratories, are presented. The results show that the procedure is effective to cause decay within the time period of the test (about 3 months) and that the decay increases with subsequent cycles. The decay observed differs in type and severity depending on the salt type and concentration and on the type of substrate. The decay types detected in the laboratories are generally representative of those observed in the field for the selected substrates. The differences in durability between the various substrates, as assessed at the end of the test, are in line with the durability expected based on field observation. The reproducibility of the results in terms of

B. Lubelli (✉) · A. Kamat
Delft University of Technology, Delft, The Netherlands
e-mail: b.lubelli@tudelft.nl

A. M. Aguilar
ETH Zurich, Zurich, Switzerland

rilem

decay type is good; some differences have been observed in terms of material loss. These are more significant in the case of NaCl contaminated specimens. Based on the results, proposals for fine-tuning of the procedure are given.

1 Introduction

Salt crystallization is a common cause of decay in porous building materials (e.g. [1–3]). Numerical models for forecasting decay due to salt crystallization are complex and therefore rarely used. Most of the time, in the practice of construction and renovation, the resistance of porous building materials to salt crystallization, when not well-known from past field experience, is assessed in the laboratory by accelerated weathering tests.

Several standards for accelerated tests are available, including a European standard (EN 12370) [4], three RILEM recommendations (RILEM 1980 [5], MS-A.1 [6], MS-A.2 [7]) and other guidelines (e.g. [8]) However, as shown by the extensive literature review published by the RILEM Technical Committee 271-ASC (Accelerated laboratory test for the assessment of the durability of materials with respect to salt crystallization) [9], these test procedures are often modified/adapted by researchers. At present, a commonly accepted testing protocol does not yet exist.

This hinders the comparison of results of different studies, as the choice of the procedure can significantly affect the outcomes, both in terms of the durability of materials and aggressiveness of different salts [10, 11].

As underlined in [9], the main limitations of existing (standard) crystallization tests are the facts that they are time consuming (e.g. [6]) and/or not realistically reproducing the transport and crystallization process occurring in the field (e.g. [4]). Often very high salt contents and extreme environmental conditions are used, altering the damage mechanism and possibly resulting in unrealistic damage types. Moreover, none of the existing standards recommends an accurate, reliable and quantitative method or technique for monitoring damage development during the test. This complicates the comparison between results.

The RILEM TC 271-ASC was set up in 2016 with the goal of overcoming the above-mentioned limitations by the development of an improved test procedure. The salt crystallization test developed by the TC 271-ASC proposes a novel approach [12], different from existing salt crystallization tests, and derived from a common approach to the durability of reinforced concrete [13]. It starts from the consideration that a certain degree of salt accumulation (pore filling) is needed [14], to initiate damage. Salt damage can thus be seen as a process developing in two stages: accumulation and propagation (Fig. 1).

The developed test procedure aims to reliably assess the differences in the durability of porous building materials against salt crystallization, accelerating the deterioration process without significantly altering its mechanism. Based on the results of the test,

K. Beck
Université d'Orléans, Orléans, France

T. De Kock
University of Antwerp, Antwerp, Belgium

J. Desarnaud
KIK-IRPA, Brussels, Belgium

E. Franzoni · E. Sassoni
Alma Mater Studiorum, Università di Bologna, Bologna, Italy

D. Gulotta
Getty Conservation Institute, Los Angeles, CA, USA

I. Ioannou
University of Cyprus, Nicosia, Cyprus

B. Menendez
CY Cergy Paris Université, Cergy-Pontoise, France

I. Rörig-Dalgaard
Technical University of Denmark, Copenhagen, Denmark

the user should be able to define a durability ranking of the different substrates with respect to salt crystallization. The test reproduces the mechanism of salt damage triggered by capillary transport of salt solution towards the evaporation surface of a material; damage by sea-salt spray is not considered. The procedure has been developed for stone and stone-like porous materials, tested as single materials (stone and brick units); the procedure can, nevertheless, with simple adaptations, be applicable to combinations of materials.

The target group for the test are laboratories in the renovation and construction sectors. Therefore, feasibility has been a main requirement in the definition of the procedure; besides, assessment methods applicable without the need for sophisticated equipment or specialized expertise have been selected.

To come to the definition of the procedure, the TC 271-ASC has carried out an extensive experimental program [15–18] supported by mathematical modelling of the transport and crystallization process [19]. Each variable of the procedure (e.g., specimen size and number, salt content, contamination procedure, weathering cycles, assessment methods) has been the subject of debate and research.

After some preliminary tests, the procedure has been assessed in a round robin test on 7 substrates at 10 laboratories. The details of the procedure and the set-up of the round robin are described in Sect. 2; the results of the test are reported in Sect. 3, organized according to the type of substrate. The effectiveness, reliability and reproducibility of the procedure are discussed in Sect. 4. Finally, proposals for fine tuning of the procedure are made (Sect. 5).
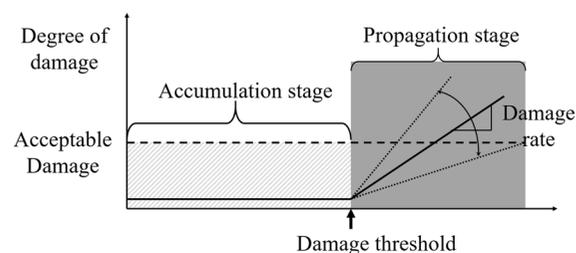
Fig. 1 Schematic representation of durability of a stone, subject to salt damage, adapted from the concept proposed by Tuutti [13] to describe the durability of reinforced concrete (adapted from [12])

2 Materials and methods

2.1 Materials

2.1.1 Selection of materials

Several substrates have been selected to be tested, including natural stones and bricks. The selected substrates are commonly used in (historic) buildings and as replacement stones in heritage sites in European countries. All stone samples selected for this study were freshly quarried. The selected materials differ in terms of moisture transport behaviour and mechanical properties and are known to have a different durability to salt decay and to show dissimilar salt decay types (Table 1 and Fig. 2). This makes it possible to validate the effectiveness of the test procedure for a wide range of substrates and to ascertain its reliability by comparing the decay type and extent, as assessed in the accelerated laboratory test, to the durability of the same substrates observed in the field. Hereafter a short description of the selected substrates is given, based on literature. In Sect. 2.1.2, the results of the characterization test performed in this research are reported.

Tuffeau stone is a soft white fine-grained sedimentary limestone [22]. It is mainly composed of calcite, quartz and opal with minor presence of micas (biotite, muscovite) and clayey minerals (glauconite, smectite). It is a very porous limestone (porosity about 45%) with a very wide pore size distribution. Its mechanical strength is about 10 MPa [22]. Tuffeau is extracted along the Loire Valley in France, and it is mainly used in this area for the construction of traditional houses and historical monuments like the famous castles of the Loire (e.g. the castle of Chambord). Tuffeau has a high susceptibility to salt decay and it is subject to many forms of degradation like scaling, flaking, exfoliation, blistering and powdering [23–25]. However, among the most common degradation patterns observed in monuments built in Tuffeau, the most severe one is spalling [26].

Massangis limestone is a white grey to yellow grey limestone from the southeastern outcrops of the Paris Basin, in the Yonne Department in Burgundy, France. It is used as building stone in old and new construction, as well as replacement stone in heritage buildings. It is quarried from the top of the Bathonian Oolithe Blanche Formation, which is a prograding oolithic facies [27]. Massangis limestone can be

Table 1 Selected substrates and their susceptibility to salt weathering, based on literature and authors' experience

Acronym	Substrate	Susceptibility to salt weathering	Common damage type in the presence of salts
MS	Massangis Clair limestone	Moderate to low	Unknown
TU	Tuffeau limestone	High	Scaling, spalling, flaking, exfoliation, blistering, powdering
MG	Migné clair limestone	High	Powdering, scaling
LE	Lecce limestone	High	Alveolization, flaking, powdering
PR	Prague sandstone	Moderate to low	Unknown
BR	Red brick	Medium	Powdering
BB	Black brick	Low	Powdering

Damage types are defined according to [20] and [21] for stone and brick, respectively

classified as an oobiosparite or bioclastic oolitic grainstone. It is composed mainly of calcite with small percentage of iron oxides and dolomite as cement [28]. Several varieties are commercialized, ranging from whitish stone (Clair) to yellowish stone (Jaune). The Jaune varieties show a more intense dedolomitization, leading to a relative increase of macroporosity as opposed to the Clair varieties that have proportionally higher microporosities. The porosity (between 10 and 17%) and compressive strength (45–105 MPa) vary considerably, depending on specific variety [29–32]. The Clair varieties are known to be less resistant to salt and freeze–thaw weathering, implying restrictions on their outdoor use [29, 33]. In this study, the Massangis Clair Nuancé, a slightly yellow tinted Clair variety, was used.

Migné stone is a white fine-grained sedimentary limestone, extracted from the quarry of Migné-Auxences, near the city of Poitiers in France. It is a porous stone (porosity about 28–30%) with a unimodal pore size distribution [32, 34]. Its compressive strength is relatively low (about 13 MPa [32]). Migné stone is used as a building and decorative material in France. The stone is reported to be susceptible to frost and salt crystallization decay [32], showing granular disintegration and scaling [35].

Lecce limestone is a lithotype widely diffused in historical buildings in southern Italy (Salento area), where it was employed for both structural and decorative elements (due to its easy carving, it was widely used in baroque architecture). It is a biocalcarenite, including a strong presence of marine fossils of different sizes, yellowish in colour, and exhibiting a

quite homogeneous composition with approximately 95% calcite and a minor presence of phosphatic minerals (fluorapatite). The porosity of this stone varies between 30 and 43 vol% and its compressive strength is about 16–22 MPa (minimum and maximum values ranging between 10 and 30 MPa) [36]. Lecce stone is highly vulnerable to deteriorating agents and salts in particular [37], suffering from decay patterns mainly including alveolization, powdering and flaking.

Mšené "Prague" sandstone (henceforth referred to as Prague) is a white-light grey psammitic rock extracted from the Mšené-lázně quarry (Czech Republic) and used in historic buildings including the S. Vitus Cathedral, Charles' Bridge [38] and the Prague Castle [39]. Quartz is the main mineralogical phase as sub-oval clasts accounting for more than 95% of its composition. Accessory minerals include muscovite and feldspar. Minor non-expanding clay, including kaolinite, can also be present [39]. This stone has a high porosity (about 31 vol%) with coarse pores [39, 40]. The stone is reported to have a good resistance to weathering, despite its relative low mechanical strength (21.7–33 MPa) [39, 40].

Next to the mentioned natural stones, two brick types have been tested.

Red Neutral is a classical red fired-clay brick used for traditional private homes and larger constructions. Characteristic of this red fired-clay brick is the use of non-calcareous clay, which prior to firing consists of less than 1% $CaCO_3$. Next to the non-calcareous clay, sand is added for the production of this brick; both raw materials originate from Flensburger Förde, Jutland,

Denmark. The bricks are fired at around 1000 °C. According to the producer datasheet, this brick has a compressive strength of 20 MPa and the porosity is determined to be 34% [41]. Red Neutral holds the Danish class of exposure MX3.2 and MX4; meaning resistant to both water and salt exposure, suitable for use in coastal areas and in the vicinity of roads subject to de-icing during the winter period (not significant amounts of sulphates).

Black Beauty is a modern fired-clay brick, a new product with a non-traditional appearance, used for private homes and larger constructions. The core of the material appears brown; due to a short exposure to high temperature ($T > 1000$ °C) during the firing process, the surface appears black and glazed. According to the producer datasheet, this brick has a compressive strength of 20 MPa and the porosity is determined to be 32% [41]. Black Beauty currently holds the Danish class of exposure MX3.2 and MX4 and is thereby considered resistant to both water and salt exposure.

2.1.2 Characterization of materials

The main physical and mechanical properties of the selected substrates were assessed in the laboratory before the start of the test.

The open porosity and pore size distribution were measured by Mercury Intrusion Porosimetry (MIP). The water absorption by capillarity at atmospheric pressure was measured in threefold on cores of 50 mm diameter and 50 mm height according to EN 1925—Natural stone test methods—Determination of water absorption coefficient by capillarity [42]. The Water Absorption Coefficient (WAC), i.e. the slope of the first, linear part of the absorption curve, was calculated. Additionally, the Capillary Moisture Content (CMC) was measured. The CMC is defined as the water content at the end of the first stage of water absorption and it is determined as the point of intersection of straight lines drawn through the first and second stages of water absorption on a $t^{1/2}$ plot.

All results are summarized in Table 2. As shown in Fig. 3, the selection of substrates includes materials with a similar porosity and different WAC, as well as substrates with similar WAC and different open porosity.

2.2 Test procedure

The test procedure used has been defined by the TC 271-ASC and it reproduces the mechanism of salt damage triggered by capillary transport of salt solution towards the evaporation surface of a material. The procedure consists of an accumulation phase, aiming at accumulating the salt in a thin layer of material just beneath the evaporation surface, and a propagation phase, aiming at developing salt crystallization damage (see Sects. 2.2.4 and 2.2.5). For more details on the procedure and the reason of the choices, please refer to [43].

2.2.1 Specimens

Cylinders of 50 ± 0.5 mm diameter and 50 ± 0.5 mm height have been used. In the case of natural stone, cores were drilled out of larger blocks, with the direction of drilling perpendicular to the bedding planes of the stone. In the case of the brick, cores were drilled through the stretcher face of the brick units, in such a way that the surface usually exposed can be the test surface. After drilling, the cores were brushed to remove debris and dried at 40 ± 5 °C. The lateral side of the specimen was sealed using paraffin film; additionally, textile tape was used on top of the paraffin film to secure it.

2.2.2 Salt types and concentration of solutions

Sodium sulphate and sodium chloride solutions, both as single salts, were used to contaminate the specimens. These two salts were selected as they are very common in the field and known for causing severe damage.

For each salt, two solution concentrations were used: 1 wt% and 5 wt% for sodium sulphate and 5 wt% and 10 wt% for sodium chloride (expressed as weight NaCl/weight solution). The solution concentrations were decided with the aim of having a high, but still realistic salt content in the material (see also [16, 43, 44] for further details).

2.2.3 Specimen preparation and contamination

The specimens were sealed along their circumference with paraffin film, after pre-heating them in an oven at 50 °C for 10 min to achieve better adherence. The

Table 2 Physical properties of the substrates as determined in this research

Acronym	Open porosity (vol%)	Density (kg/m³)	WAC (kg/m² s^0.5)	CMC (wt%)
MS	13	2230	0.05	4.8
TU	50	1290	0.50	31.7
MG	32	1810	0.28	14.7
LE	34	1750	0.10	10.9
PR	28	1850	1.07	12.7
BR	34	1760	0.24	12.1
BB	32	1800	0.28	12
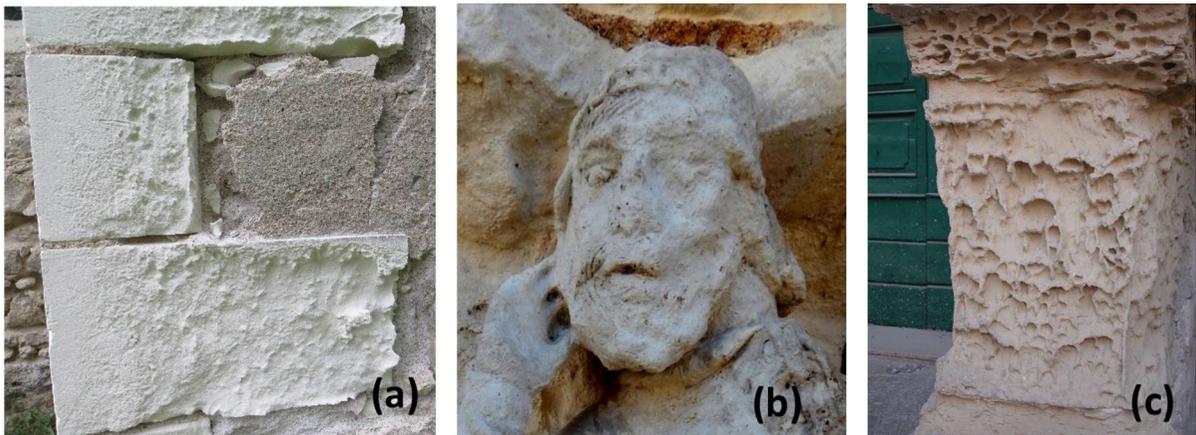
Fig. 2 Decay patterns in the presence of salts in some of the selected substrates; **a** powdering in Tuffeau, chapel of Maurepas, Chambord (F) (photo, courtesy of Kevin Beck); **b** powdering and scaling in Migné stone, Notre-Dame-la-Grande, Poitiers (F) (photo, courtesy of Veronique Verges-Belmin); **c** Alveolization and powdering in Lecce stone, Church of S. M. del Carmelo, Nardo' (I); (photo, courtesy of Rob van Hees)
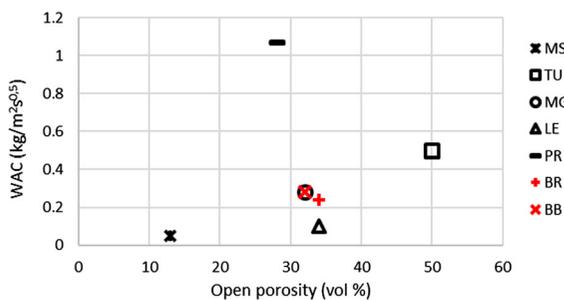
Fig. 3 Open porosity and Water Absorption Coefficient (WAC) of the selected substrates

paraffin film extended ca. 5 mm above the top surface of the specimens, to avoid efflorescence and/or material debris, produced during the test, falling down. Textile tape (water resistant and water vapour tight) was used to secure the ends of the paraffin film and ensure sealing tightness during the entire test.

Before contamination, the specimen mass was stabilized for 4 h at room conditions (22 ± 2 °C/ 45 ± 15% RH). Contamination with salt solution occurred via capillary absorption. An amount of solution, equal to the capillary moisture content (CMC) of the material, was poured into a container. The specimen was then placed in the container with its bottom surface, i.e., through the surface opposite to the evaporation surface, in contact with the solution.

Immediately after the full absorption of the required salt solution, the bottom surface of the specimens was sealed with paraffin film and tape.

2.2.4 Accumulation phase

The accumulation phase consisted in drying the specimens contaminated with salt solution at 40 °C/ 15 ± 5% RH, with very low air flow, until 80% of the absorbed water had evaporated.

The low air flow was chosen in order to limit variations between the test conditions at different labs. In order to reduce the air flow, the specimens were placed in a box, closed with textile or Japanese paper. The temperature and RH were monitored during the test, to be sure that the desired temperature and RH conditions were reached and maintained.

At the end of the drying period, the presence of damage and/or efflorescence was photographically recorded and described according to the methodology reported in Sect. 2.2.6.

2.2.5 Propagation phase

The propagation phase consisted of repeated dissolution and crystallization cycles of the salts present in the pores of the materials. These cycles were different for Na_2SO_4 and NaCl contaminated specimens, as the damage mechanism of these salts is triggered by different conditions [9].

In the case of Na_2SO_4 contaminated specimens, the propagation phase consisted of 4 cycles, each with a duration of 2 weeks. Each 2-week cycle consisted of:

- Cooling of the specimens for 4 h at room conditions ($T = 22$ °C ± 2 at 45% RH $\pm 15\%$)
- Removal of the sealing from the bottom surface.
- Re-wetting with water (80% of the initial water weight) by capillarity from the bottom surface at room conditions ($T = 22$ °C ± 2 at 45% RH $\pm 15\%$). Sealing of the bottom surface with paraffin film.
- Drying at room conditions ($T = 22$ °C ± 2 at 45% RH $\pm 15\%$) up to 24 h from the start of the re-wetting.
- Drying for 312 h (13 days) at 40 °C/15 $\pm 5\%$ RH

The weight of the specimens was recorded at the end of each 2-week cycle.

In the case of NaCl contaminated specimens, the propagation phase consisted of 3 cycles; each cycle had a duration of 3 weeks. Each 3-week cycle consisted of:

- 24 h hygroscopic adsorption at 20 °C/95% RH
- 12 h drying at 20 °C 50% RH
- 44 h drying at 40 °C 15 $\pm 5\%$ RH
- 24 h hygroscopic adsorption at 20 °C/95% RH
- 12 h drying at 20 °C 50% RH

- 44 h drying at 40 °C 15 $\pm 5\%$ RH
- 24 h hygroscopic adsorption at 20 °C/95% RH
- 12 h drying at 20 °C 50% RH
- 44 h drying at 40 °C 15 $\pm 5\%$ RH
- 4 h cooling at room conditions (22 ± 2 °C/ $45 \pm 15\%$ RH). Removal of the sealing from the bottom surface.
- Re-wetting with water from the bottom surface with 50% of the water amount used for the initial contamination. Sealing of the bottom surface with paraffin film.
- 1 h storage of the specimens at RH > 95% (in order to allow for salt dissolution)
- 264 h drying at 40 °C/15 $\pm 5\%$ RH.

The weight of the specimens was recorded at the end of each 3-week cycle.

2.2.6 Assessment method

The development of the decay on the surface of the specimens was monitored by visual observations and photographically documented at regular intervals during the test: at the end of the accumulation phase and at the end of each cycle in the propagation phase. Pictures of the specimens were taken at 90° and at 45° angles with respect to the evaporation surface. The damage type was described following the terminology of the ICOMOS [20] and MDCS [21] atlases.

At the end of the propagation phase, the paraffin film was removed and the material loss was quantified by brushing the surface with a soft brush and collecting the loose debris (material and salt efflorescences). The weight of the debris was recorded before and after dissolution and filtration of the salts; in this way the actual material loss was determined. Besides, any damage occurring below the surface, such as cracks parallel to the surface, was recorded.

2.2.7 Round robin test

Ten laboratories were involved in the round robin test, each of them testing a selection of substrates, with one or two salt types. The complete scheme of the round robin test is given in Table 3. Overlap of at least 2 labs for each tested substrate/salt combination has been considered, in order to allow for comparison; next to this, the interest of a lab for a specific substrate (e.g., as

commonly used in the country) has been taken into account.

3 Results

In the following subsection, the results for each of the substrates are discussed and some examples of the decay observed are given. Figure 4 provides an overview of the material loss measured at the end of the test; please refer to the supplementary material for the pictures of the evolution of the decay during the test for all substrates.

3.1 Tuffeau limestone

Tuffeau specimens contaminated with Na_2SO_4 showed chromatic alteration (darkening), visible already at the end of the accumulation phase, for both salt solution concentrations. Further, no damage was observed in specimens contaminated with 1 wt% Na_2SO_4 solution.

Specimens contaminated with 5 wt % solution showed efflorescence and loss of cohesion, including blistering, scaling, powdering and exfoliation (Fig. 5a). The damage started in the first propagation cycles and increased with subsequent cycle. At the end

of the test, an average material loss of 0.51 g (standard deviation 0.26) was measured (Fig. 4). The damage type was similar between the labs and representative of the decay type observed in the field.

Tuffeau specimens contaminated with NaCl showed similar decay type and severity at the different labs. Surface damage developed in the form of powdering (Fig. 5b); additionally, a crack, parallel to the evaporation surface, appeared during the test in most of the specimens; in some specimens this developed in detachment of the outer layer (Fig. 5c). The damage types were similar for both salt concentrations, but the severity of the damage was higher at higher salt concentration. While powdering is a common damage in NaCl contaminated Tuffeau in the field, cracks parallel to the evaporation surface and detachment of the outer layer are not generally observed. This suggests that the damage might be an artefact of the test procedure: the paraffin film nearby the evaporation surface might have detached/loosened during the test leading to evaporation and subsequent salt crystallization at the lateral sides.

The material loss measured at the end of the test in NaCl contaminated specimens showed a large variation, mainly related to the occurrence of the detachment of the outer layer. The variation of material loss

Table 3 Overview of laboratories involved in the round robin test and substrate/salt combination tested at each laboratory

|	Massangis	Tuffeau	Fired-clay brick, Red	Fired-clay brick, Black	Migné	Lecce stone	Prague sandstone
LAB_1		NaCl, Na_2SO_4					NaCl, Na_2SO_4
LAB_2	NaCl, Na_2SO_4			Na_2SO_4	NaCl, Na_2SO_4		
LAB_3	NaCl, Na_2SO_4		Na_2SO_4				NaCl, Na_2SO_4
LAB_4	NaCl, Na_2SO_4	NaCl, Na_2SO_4			NaCl, Na_2SO_4		
LAB_5		Na_2SO_4	Na_2SO_4	Na_2SO_4			
LAB_6			Na_2SO_4		Na_2SO_4		
LAB_7		NaCl, Na_2SO_4			NaCl, Na_2SO_4	NaCl	
LAB_8	Na_2SO_4	Na_2SO_4					Na_2SO_4
LAB_9	NaCl					NaCl	NaCl
LAB_10				Na_2SO_4			
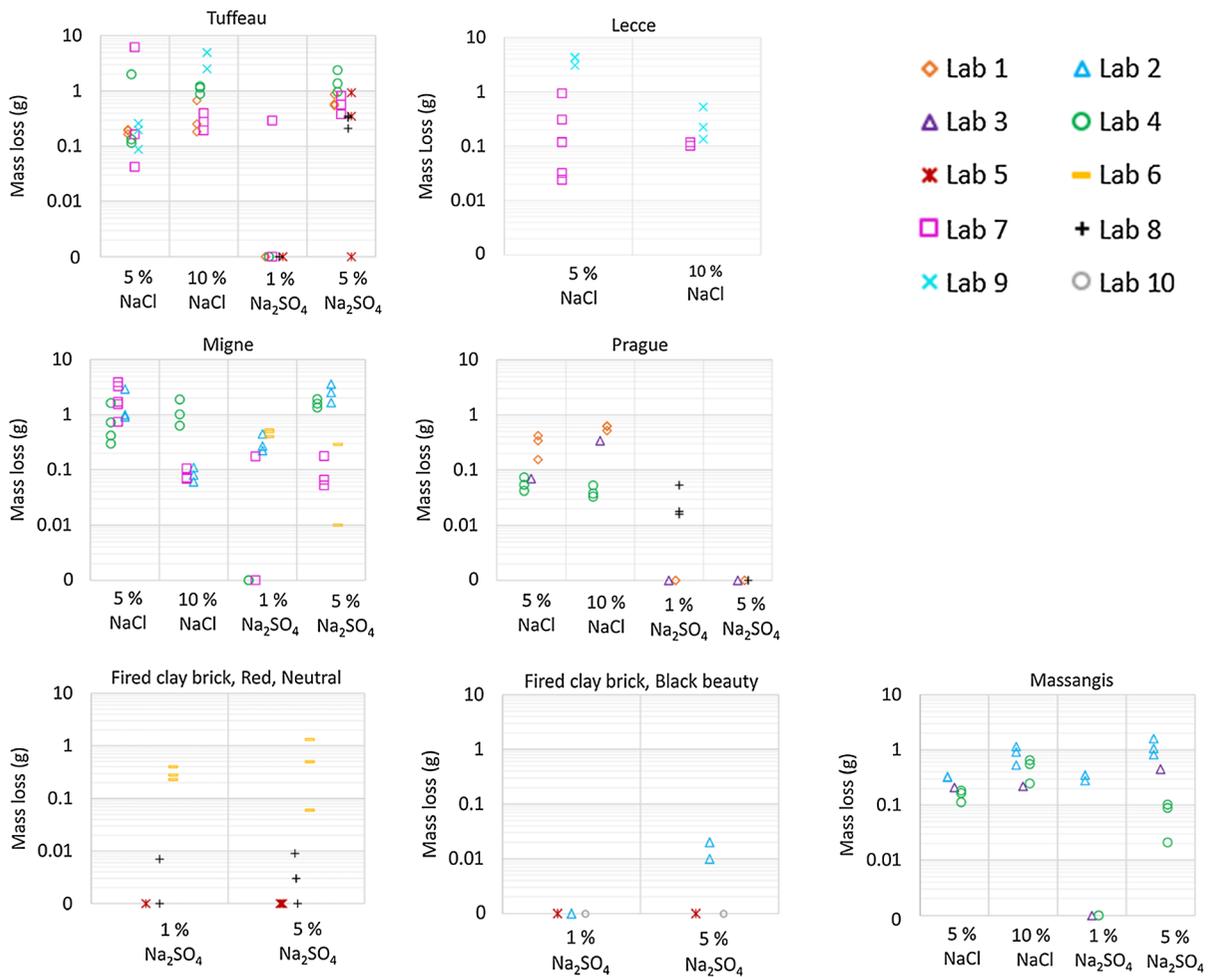
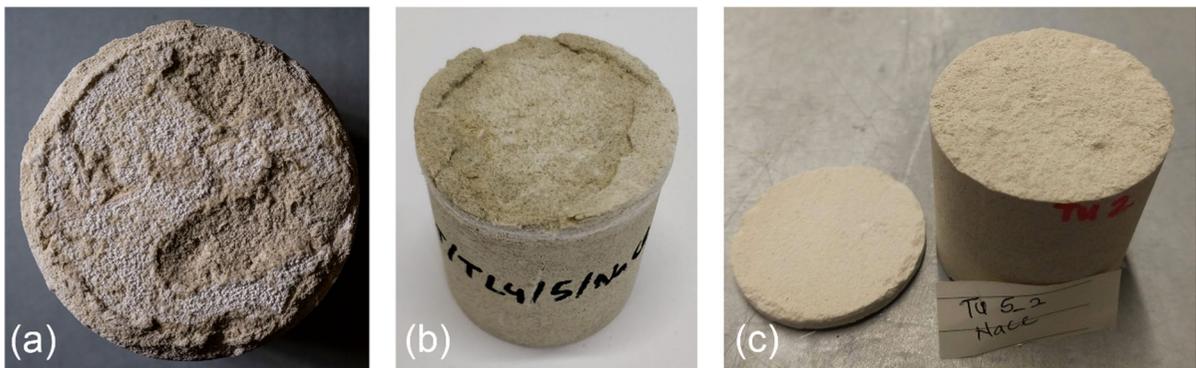**Fig. 4** Material loss in the different substrates at the end of the test

Fig. 5 a Decay in Tuffeau specimen contaminated with 5 wt% Na_2SO_4 at the end of the test, after brushing off the evaporation surface; **b** decay in Tuffeau specimen contaminated with 10 wt% NaCl at the end of the test, after brushing off the evaporation surface; **c** spalling of the outer layer of Tuffeau specimen contaminated with 5 wt% NaCl, after brushing off the evaporation surface

within the same lab is comparable to the variation across different labs (Fig. 4).

3.2 Migné limestone

Migné specimens contaminated with 1 wt% Na_2SO_4 presented chromatic alteration, powdery and/or cauliflower-like efflorescence, and loss of cohesion in the form of scaling/flaking and granular disintegration (Fig. 6a). Damage initiated in the first propagation cycle and increased with subsequent cycles. With 5 wt% Na_2SO_4, chromatic alteration, efflorescence and progressive loss of cohesion were also observed (Fig. 6b). However, in at least one case, the mass loss recorded due to powdering/chalking/flaking at the end of the test was surprisingly less, compared to the test with 1 wt% Na_2SO_4; this was attributed to the fact that salt crust remained attached to the surface of the specimens. Figure 4 depicts the amount of material loss with the use of 1 wt% and 5 wt% Na_2SO_4 concentration in the various labs involved in the testing of this substrate. The results show considerable variation, both between labs and within each lab, mainly due to the presence of the salt crust on the surface of the test specimens, which inhibited (at least temporarily) material loss and encouraged cryptoflorescence and pore clogging.

Migné specimens contaminated with NaCl at 5 wt% and 10 wt% concentration showed a similar type of damage: loss of cohesion in the form of powdering, scaling and spalling of the surface layer (Fig. 6c). The amount of material loss varied (Fig. 4), depending on whether the surface layer detached or not. At two of the three laboratories involved,

specimens contaminated with 5 wt% solution showed more severe decay than specimens contaminated with 10 wt% solution. This is most probably due to incomplete drying of the specimens with the higher salt load during the cycles in the propagation stage.

The powdering and scaling observed in the various laboratories are similar to the decay patterns observed in the field in the presence of these salts. However, the spalling recorded in the case of NaCl contaminated specimens is unusual in the field for this type of stone and salt combination.

3.3 Massangis limestone

Massangis samples contaminated with Na_2SO_4 showed powdering, concentrated at the borders of the evaporation surface, and a salt crust (Fig. 7a, b). The damage started to appear at the second re-wetting period in samples contaminated with 5 wt% solution and in the third cycle in those contaminated with the 1 wt% solution. The samples with the highest salt concentration had the highest material loss (Fig. 4).

Massangis samples contaminated with NaCl showed surface damage in the form of powdering and granular disintegration (Fig. 7c), mainly starting at the last re-wetting cycle. The weathering was more severe at the borders of the evaporation surface. The amount of material loss was low for the samples contaminated with the 5 wt% solution; a higher material loss was measured for the samples contaminated with the 10 wt% solution (Fig. 4).

Fig. 6 **a** Decay and efflorescences in Migné specimens contaminated with 1 wt% Na_2SO_4 at the end of the test, before brushing off the evaporation surface; **b** decay in Migné specimen contaminated with 5 wt% Na_2SO_4 at the end of the test, before brushing off the evaporation surface; **c** decay in Migné specimen contaminated with 5 wt% NaCl at the end of the test, after brushing off the evaporation surface

Fig. 7 **a** Salt crust in Massangis specimens contaminated with 5 wt% Na_2SO_4; **b** detail of salt crust on Massangis specimen contaminated with 1 wt% Na_2SO_4 after brushing off the evaporation surface; **c** decay in Massangis specimen contaminated with 10 wt% NaCl at the end of the test, after brushing off the evaporation surface
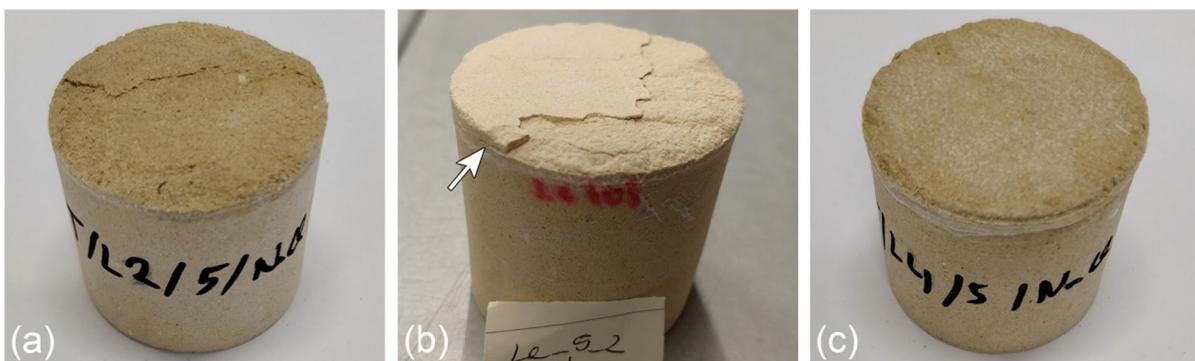
3.4 Lecce stone

Lecce stone was tested only with NaCl. Specimens contaminated with NaCl showed a thin layer of efflorescence at the end of the accumulation stage, without visible damage. The damage appeared after the 1st propagation cycle, and it increased with every cycle.

In specimens contaminated with 5 wt% solution, damage occurred in the form of scaling and flaking (Fig. 8a). At the end of the propagation phase, the specimens made a hollow sound when gently knocking on their surface, suggesting a detachment of the top layer. In some cases, this top layer detached during the assessment of mass loss at the end of the test (Fig. 8b). This explains the large differences in material loss observed between specimens and between labs (Fig. 4).

Specimens contaminated with 10 wt% NaCl showed mainly granular disintegration (Fig. 8c). The damage type and mass loss were comparable between labs. A thin layer of cryptoflorescence accumulated a few millimetres underneath the surface, which can be observed on the lateral side. When comparing specimens contaminated with 5 wt% and 10 wt% NaCl solution, the damage was more severe, in terms of mass loss, in the specimens with the lower salt content. This might be due to the not complete drying of the specimens during the adsorption/drying cycles.

The type of damage is similar across the two labs that took part in the round robin test and resembles that present in the field on this stone; however, Lecce stone often shows alveolization too.

Fig. 8 **a** Decay in Lecce stone specimens contaminated with 5 wt% NaCl at the end of the test, after brushing off the evaporation surface; **b** decay in Lecce stone specimen contaminated with 5 wt% NaCl at the end of the test, after brushing off the evaporation surface (arrow indicates a crack); **c** decay in Lecce stone specimen contaminated with 10 wt% NaCl, at the end of the test, after brushing off the evaporation surface

3.5 Prague sandstone

Both Na_2SO_4 concentrations induced visible chromatic alterations of the Prague sandstone specimens at the end of the accumulation phase, consisting of increased colour saturation and shifting of the original greyish hue of the stone towards a brown-yellow appearance (Fig. 9a). Overall, the magnitude of such alterations increased as the test progressed, leading to the formation of irregular brow-coloured stains at the end of the last propagation phases. The final response of the stone seemed to be affected by the salt concentration. In most cases, the 1 wt% solution only determined chromatic alteration, staining and the presence of salt crust (Fig. 9b), whereas the 5 wt% concentration also induced a very limited loss of material due to mild granular disintegration. In one case (Lab 8) the lowest salt concentration was also associated with limited loss of material. The results obtained by the different laboratories are consistent as for the type of alteration and deterioration observed.

Prague sandstone specimens contaminated with NaCl developed powdery efflorescences irregularly covering the evaporation surface at the end of the accumulation phase with both salt concentrations. No clear sign of deterioration was observed at this stage. After the first propagation cycle and during the following ones, the amount of surface crystallization decreased. Both salt concentrations induced surface changes due to persisting efflorescences, and granular disintegration was observed only at the end of the last cycle. The material loss associated with the 10 wt% concentration was generally higher than with the 5 wt% (Fig. 4). In some specimens, damage in the form of blistering was also observed after contamination with the highest salt solution concentration (Fig. 9c). The results obtained by the different laboratories are consistent as for the type of alteration and deterioration observed.

3.6 Red brick

Red brick specimens contaminated with Na_2SO_4 exhibited no efflorescence at the end of the accumulation phase. In the propagation phase, a thin layer of efflorescence appeared on a large part of the surface, both in the case of 1 wt% and 5 wt% salt contamination (Fig. 10a). However, the mass loss due to the propagation phase found at the three laboratories involved in the testing of this substrate was different. In two laboratories, no damage was observed (Fig. 10b), while in another laboratory damage in the form of powdering and crumbling was observed and material loss was recorded (Fig. 10c); the material loss was higher in the case of the higher salt concentration (Fig. 4).

The different results obtained were ascribed to the fact that the specimens were core drilled from different bricks, thus being affected by the heterogeneity among bricks, even when these are coming from the same batch.

3.7 Black brick

Exposure of the fired-clay brick of the type Black Beauty, here named Black brick, to Na_2SO_4 accumulation and subsequent crystallization cycles only resulted in minor changes. This was expected due to
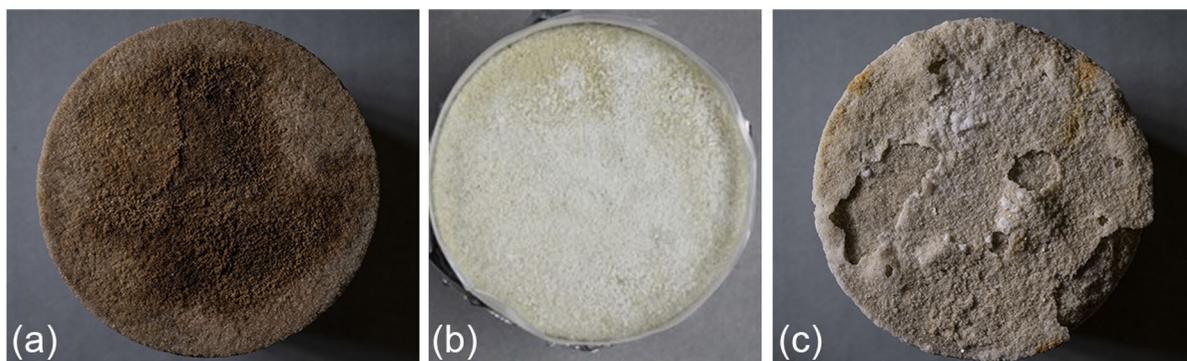
Fig. 9 **a** Decay in Prague stone specimens contaminated with 5 wt% Na_2SO_4 at the end of the test, after brushing off the evaporation surface; **b** salt crust in Prague stone specimen contaminated with 1 wt% Na_2SO_4; **c** decay in Prague stone specimen contaminated with 10 wt% NaCl, at the end of the test, after brushing off the evaporation surface

Fig. 10 a Decay and salt crust on Red brick specimens contaminated with 5 wt% Na_2SO_4 at the end of the test, after brushing off the evaporation surface; **b** surface of Red brick specimen contaminated with 1 wt% Na_2SO_4, at the end of the test, before brushing off the evaporation surface **c** decay in Red brick specimen contaminated with 5 wt% Na_2SO_4, at the end of the test, before brushing off the evaporation surface

a heat treatment of the exposed surface resulting in a melting of the outer clay minerals and in consistence with the producer's classification of the material as being suitable for environments in coastal areas and in the vicinity of roads subject to de-icing during the winter period.

In contrast to other test materials in the present work, no chromatic changes in the material were observed except for the presence of the salts themselves. In the specimens exposed to 1% Na_2SO_4 solution, minor efflorescence was observed during the crystallization cycles in cracks and on the exposed surface (Fig. 11a), whereas the efflorescence was more pronounced for the specimens contaminated with 5% Na_2SO_4 solution (Fig. 11b). A minor material loss was registered at two of the three laboratories performing the test (< 1 mg) (Fig. 4) and in the third lab, minor material loss was visually observed

(Fig. 11c). Such minor material losses are challenging to document. In general, the results observed at the different labs, in regards to both material loss and efflorescence, were consistent.

4 Discussion

4.1 Test effectiveness (in general, for all substrates, using examples)

The test can be considered effective if it can produce damage and the severity of the damage differs depending on the tested material (in such a way that materials can be ranked according to their different durability) and salt concentration (the higher salt concentration is expected to lead to more severe damage). Besides, the damage should appear in the
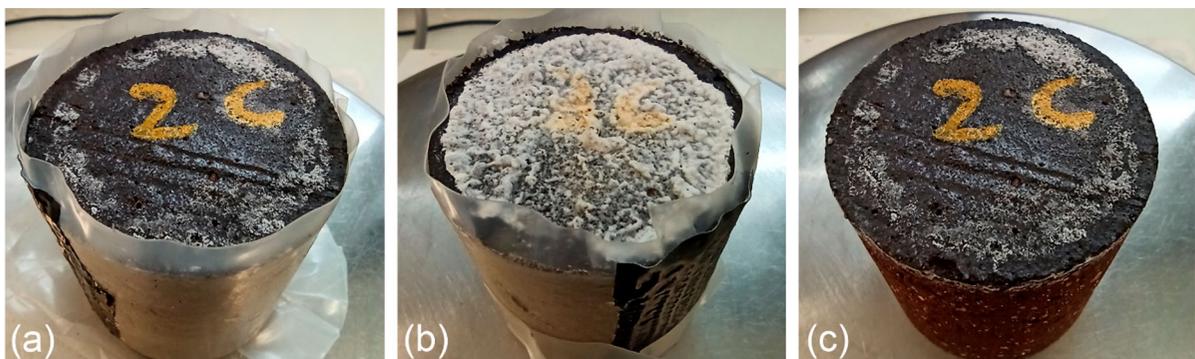
Fig. 11 a Limited efflorescence on Black brick specimens contaminated with 1 wt% Na_2SO_4 at the end of the test, before brushing off the evaporation surface; **b** more pronounced efflorescences on Black brick specimens contaminated with 5 wt% Na_2SO_4, at the end of the test, before brushing off the evaporation surface; **c** detail of Black brick specimen contaminated with 5 wt% Na_2SO_4, at the end of the test, after brushing off the evaporation surface

(a)

(b)
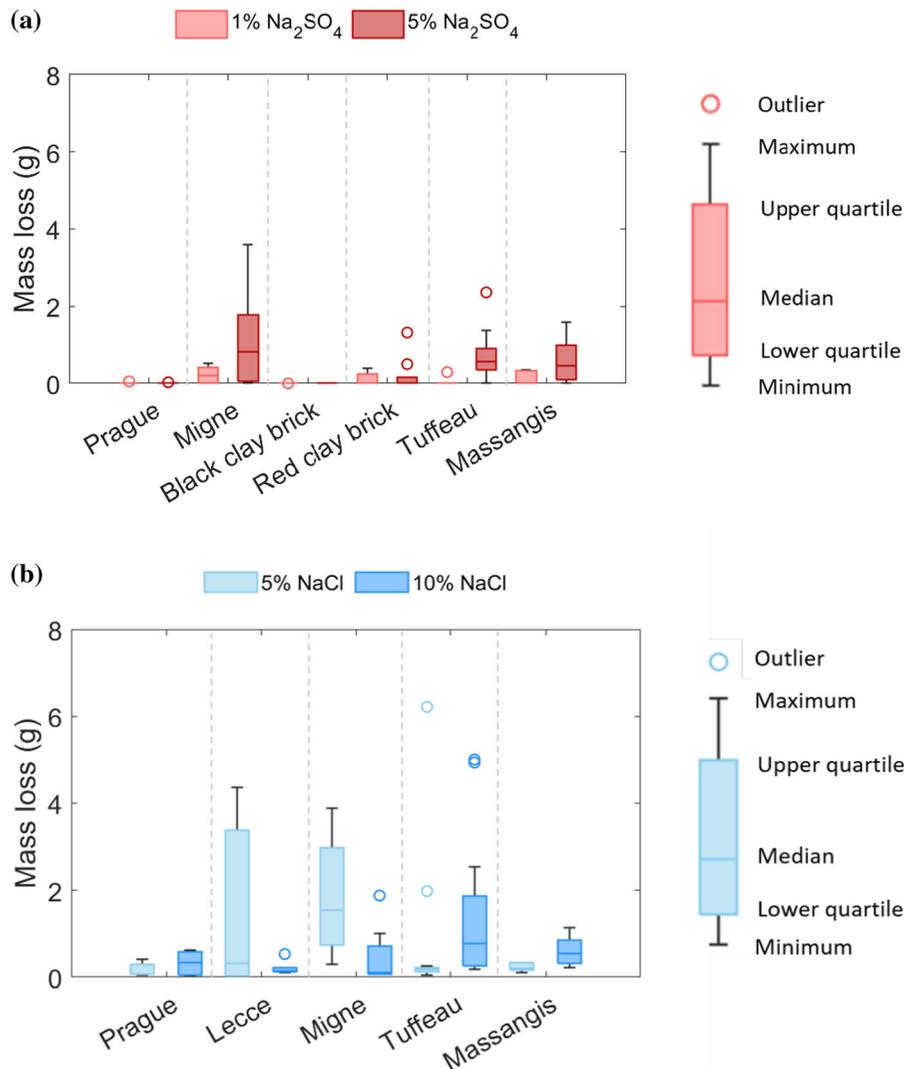
Fig. 12 Material loss measured at the end of the test at the different labs on the tested substrates contaminated with Na_2SO_4 (**a**) and NaCl (**b**)

propagation phase only and increase with the number of cycles.

In the case of specimens tested with sodium sulphate, specimens contaminated with 1 wt% solution did not show any damage. Specimens contaminated with 5 wt% solution, showed damage in the propagation phase and this damage increased with subsequent wet-dry cycles. Some substrates were more damaged than others. Therefore, it can be concluded that 5 wt% Na_2SO_4 solution concentration is effective, whereas 1 wt% concentration is too low. It is therefore proposed to use 5 and 10 wt% concentrations in the further development of the test.

In the case of specimens contaminated with sodium chloride, damage was observed for both 5 wt% and 10 wt% solution concentrations; however, in some cases, the damage in the specimens with higher salt content was less than that in specimens with lower salt content. This has been attributed to incomplete drying, and thus limited re-crystallization of the salts, during the wet-dry cycles. Because of this reason, it is therefore proposed to re-wet the specimens with only 30% of the water amount used in the contamination phase (instead of 50%). Besides, in order to facilitate the dissolution of the salt during re-wetting, a storing period at room temperature can be included after re-wetting.

4.2 Test reliability

The test can be considered reliable if the severity and type of damage obtained are similar to that observed in the field. For what concerns the severity of the damage, generally substrates known to be susceptible to salt damage showed more severe damage than those considered to be salt resistant. This is true in the case of both salts.

The type of damage in contaminated specimens is generally representative of that observed in the field. Sodium chloride laden specimens sometimes showed spalling of a few mm layer (or cracks parallel to the evaporation surface, preluding at spalling); this damage type is not typical for NaCl, which generally causes loss of cohesion (powdering, sanding, scaling etc.) and it can be an artifact of the specimen preparation (the paraffin film sealing might have loosened up nearby the evaporation surface, leading to evaporation though the sides and crystallization) or of the test procedure itself (accumulation of salt right beneath the evaporation surface followed by dissolution and crystallization cycles leading to concentrated stresses). Based on these results, it is proposed to use a different specimen preparation, able to avoid loosening of the paraffin film layer.

4.3 Test reproducibility

Figure 12 reports the damage type and the material loss observed at the different labs. In general, the reproducibility of the results in the case of sodium sulphate contaminated specimens is quite good. In the case of sodium chloride contaminated specimens, a larger variation is observed: this is probably due both to the more complex procedure, which increases the chances of small differences in conditions between labs, and the occurrence of cracks parallel to the evaporation surface, leading to spalling at different moments of the test, depending on the intrinsic variability between specimens of the same type.

5 Conclusions

A procedure for the assessment of the differences in the durability of building materials under the influence of salt (NaCl and Na_2SO_4) crystallization cycles has been developed by the RILEM TC 271-ASC. In this study the effectiveness, reliability and reproducibility of this procedure have been assessed on 7 stones and brick substrates, at 10 laboratories.

The results show that the procedure is effective to cause decay within the time period of the test (about 3 months) and that the decay increases with subsequent cycles. The decay observed differs depending on the salt concentration used and on the type of substrate.

The decay types detected in the labs are in general representative of those observed in the field for the selected substrates. The durability of the different substrates, as assessed at the end of the test, is in line with the durability expected based on field observation.

The reproducibility of the results in terms of decay type is good; some differences have been observed in terms of material loss. These are more significant in the case of NaCl contaminated specimens. Nonetheless, the comparative evaluation of the NaCl results still allows for a relative ranking of the durability of the tested substrates across the different laboratories.

Based on this first round robin test, some improvements to the procedure have been proposed and will be considered in a second round robin test, which is ongoing at the moment of writing:

- Specimen preparation will be improved to avoid loosening of the paraffin film at the top of the specimen.
- Higher Na_2SO_4 concentrations will be used (5 wt% and 10 wt% instead of 1 wt% and 5 wt%).
- A lower amount of water (30% instead of 50%) will be used to re-wet NaCl contaminated specimens during the propagation phase, to ensure full drying before the start of RH cycles.
- A period of storage of specimens at ambient temperature after re-wetting will be added to facilitate the dissolution of the salts.
- The length of the propagation cycles of Na_2SO_4 specimens will be longer (3 weeks instead of 2), to ensure full drying of the specimens before re-wetting.
- 4 cycles will be used in the propagation phase, for both NaCl and Na_2SO_4 contaminated specimens.

The test procedure, as developed until now, is suitable for application on single materials (brick or stone units), with a quite high open porosity (ranging

between 13 and 50%) and WAC between 0.05 and 1.07 kg/m^2 s$^{1/2}$). In the future, the procedure can be adapted to consider a combination of materials (mortar/brick/stone) as well.

Declarations

References

1. Goudie A, Viles H (1997) Salt weathering hazards. Wiley
2. Charola AE (2000) Salts in the deterioration of porous materials: an overview. J Am Inst Conserv 39:327–343. https://doi.org/10.1179/019713600806113176
3. Doehne E (2001) Salt weathering: a selective review. Nat Stone Weather Phenom Conserv Strateg Case Stud 205:51–64. https://doi.org/10.1144/GSL.SP.2002.205.01.05
4. CEN (1999) EN 12370—Natural stone test methods—Determination of resistance to salt crystallization
5. RILEM TC 25-PEM (1980) Recommended tests to measure the deterioration of stone and to assess the effectiveness of treatment methods
6. RILEM TC 127-MS (1998) MS-A.1 determination of the resistance of wallettes against sulphates and chlorides. Mater Struct 31:2–9. https://doi.org/10.1007/bf02486406
7. RILEM TC 127-MS (1998) MS-A.2 uni-directional salt crystallization test for masonry units. Mater Struct 31:10–11. https://doi.org/10.1007/BF02486407
8. WTA (2005) Merkblatt 2–9–04/D -Sanierputssysteme (Renovation mortar systems)
9. Lubelli B, Cnudde V, Diaz-Goncalves T et al (2018) Towards a more effective and reliable salt crystallization test for porous building materials: state of the art. Mater Struct Constr. https://doi.org/10.1617/s11527-018-1180-5
10. Benavente D, García Del Cura MA, Bernabéu A, Ordóñez S (2001) Quantification of salt weathering in porous stones using an experimental continous partial immersion method. Eng Geol. https://doi.org/10.1016/S0013-7952(01)00020-5
11. Manohar S, Chockalingam N, Santhanam M (2021) Experimental comparison between salt weathering testing procedures on different types of bricks. J Mater Civ Eng 33:1–9. https://doi.org/10.1061/(asce)mt.1943-5533.0003936
12. Flatt RJ, Mohamed NA, Caruso F et al (2017) Predicting salt damage in practice: a theoretical insight into laboratory tests. RILEM Tech Lett 2:108–118. https://doi.org/10.21809/rilemtechlett.2017.41
13. Tuutti K (1982) Corrosion of steel in concrete, CBI Forsk. 824. http://lup.lub.lu.se/record/3173286
14. Flatt RJ, Caruso F, Sanchez AMA, Scherer GW (2014) Chemo-mechanics of salt damage in stone. Nat Commun 5:4823. https://doi.org/10.1038/ncomms5823
15. Nunes C, Sanchez Aguilar AM, Godts S et al (2021) Towards a more effective and reliable salt crystallisation test for porous building materials—experimental research on salt contamination procedures and methods for assessment of the salt distribution. Constr Build Mater 298:123862
16. Nunes C, Godts S, Sanchez Aguilar AM et al (2021) Towards a new salt crystallisation test: comparison of salt contamination procedures. In: Lubelli B, Kamat A, Quist W (eds) SWBSS2021 - Fifth International Conference on Salt Weathering og Buildings and Stone Sculptures. Delft, pp 69–77
17. Gulotta D, Gods S, De Kock T, Steiger M (2021) Comparative estimation of the pore filing of single salts in natural stone. In: Lubelli B, Kamat A, Quist W (eds) Fifth International Conference on Salt Weathering of Building and Stone Sculptures. TU Delft Open, Delft, pp 79–88
18. Kyriakou L, Aguilar Sanchez AM, Nunes C, Ioannou I (2021) Assessment of salt distribution in Maastricht and Migné limestones with the use of micro-destructive techniques. In: Lubelli B, Kamat A, Quist W (eds) SWBSS2021 - Fifth International Conference on Salt Weathering of Buildings and Stone Sculptures. TU Delft Open, Delft, pp 153–162
19. D'Altri AM, de Miranda S, Beck K et al (2021) Towards a more effective and reliable salt crystallisation test for porous building materials: predictive modelling of salt distribution. Constr Build Mater 304:124436
20. ICOMOS-ISCS (2008) Illustrated glossary on stone deterioration patterns

21. MDCS Damage Atlas. https://mdcs.monumentenkennis.nl/. Accessed 21 Jan 2022

22. Beck K, Al-Mukhtar M, Rozenbaum O, Rautureau M (2003) Characterization, water transfer properties and deterioration in tuffeau: building material in the Loire valley-France. Build Environ 38:1151–1162. https://doi.org/10.1016/S0360-1323(03)00074-X

23. Balawi M, Beck K, Janvier R, Janvier-Badosa, S. Brunetaud X (2021) Matter loss quantification and chemical analysis for the diagnosis of powdering: the case study of the chapel of Maurepas. In: Lubelli B, Kamat A, Schlangen E (eds) SWBSS2021 - Fifth International Conference on Salt Weathering of Buildings and Stone Sculptures. TU Delft Open, Delft, pp 327–335

24. Janvier-Badosa S, Beck K, Brunetaud X, Al-Mukhtar M (2014) The occurrence of gypsum in the scaling of stones at the Castle of Chambord (France). Environ Earth Sci 71:4751–4759. https://doi.org/10.1007/s12665-013-2865-2

25. Beck K, Al-Mukhtar M (2010) Evaluation of the compatibility of building limestones from salt crystallization experiments. Geol Soc Lond Spec Publ 333:111–118. https://doi.org/10.1144/SP333.11

26. Janvier-Badosa S, Beck K, Balawi M et al (2021) Analysis of spalling in tuffeau: case study of the castles of Chambord and Chaumont-sur-Loire in France. In: Lubelli B, Kamat A, Quist W (eds) SWBSS2021 - Fifth International Conference on Salt Weathering of Buildings and Stone Sculptures. TU Delft Open, Delft, pp 327–335

27. Casteleyn L, Robion P, Collin PY et al (2010) Interrelations of the petrophysical, sedimentological and microstructural properties of the Oolithe Blanche Formation (Bathonian, saline aquifer of the Paris Basin). Sediment Geol 230:123–138. https://doi.org/10.1016/j.sedgeo.2010.07.003

28. Boone MA, De Kock T, Bultreys T et al (2014) 3D mapping of water in oolithic limestone at atmospheric and vacuum saturation using X-ray micro-CT differential imaging. Mater Charact 97:150–160. https://doi.org/10.1016/j.matchar.2014.09.010

29. Noel P (1970) Les carrieres Francaises de pierre de taille. Société de diffusion des techniques du bâtiment et des travaux publics

30. WTCB (1997) Natuursteen—Tecnische voorlichting 205—Fiche nr. W510. 78

31. Honeyborne DB (1982) Building limestones of France. Department of the Environment, Building Research Establishment

32. Eslami J, Walbert C, Beaucour AL et al (2018) Influence of physical and mechanical properties on the durability of limestone subjected to freeze-thaw cycles. Constr Build Mater 162:420–429. https://doi.org/10.1016/j.conbuildmat.2017.12.031

33. Camerman C (1957) Beschrijving and gebruik in Belgie en in Nederland van de Franse witte steen. Drukkerij Hayez, Brussel

34. Borsoi G, Lubelli B, van Hees R et al (2016) Effect of solvent on nanolime transport within limestone: how to improve in-depth deposition. Colloids Surf A Physicochem Eng Asp 497:171–181. https://doi.org/10.1016/j.colsurfa.2016.03.007

35. Verges-Belmin V, Vieweger T (2018) Présentation des principes physiques régissant l'extraction des sels de la pierre, et état des connaissances sur le dessalement par bain. Le dessalement des pierres en œuvre

36. Vasanelli E, Colangiuli D, Calia A et al (2015) Ultrasonic pulse velocity for the evaluation of physical and mechanical properties of a highly porous building limestone. Ultrasonics 60:33–40. https://doi.org/10.1016/j.ultras.2015.02.010

37. Calia A, Laurenzi Tabasso M, Maria Mecchi A, Quarta G (2014) The study of stone for conservation purposes: Lecce stone (southern Italy). Geol Soc London, Spec Publ 391:139–156. https://doi.org/10.1144/SP391.8

38. Remzova M, Zouzelka R, Lukes J, Rathousky J (2019) Potential of advanced consolidants for the application on sandstone. Appl Sci. https://doi.org/10.3390/app9235252

39. Pavlík Z, Michálek P, Pavlíková M et al (2008) Water and salt transport and storage properties of Mšené sandstone. Constr Build Mater 22:1736–1748. https://doi.org/10.1016/j.conbuildmat.2007.05.010

40. Vejmelková E, Keppert M, Reiterman P, Černý R (2013) Mechanical, hygric and thermal properties of building stones. WIT Trans Built Environ 131:357–367. https://doi.org/10.2495/STR130301

41. Simonsen CP, Rörig-Dalgaard I (2020) Quantifying surface deterioration: exemplified on fired clay bricks. In: Kubica J, Kwiecień A, Bednarz Ł (eds) Proceedings of the 17th international brick and block masonry conference (IB2MaC 2020). Krakov, pp 296–303

42. CEN (1999) NEN-EN 1925—Natural stone test methods—determination of water absorption coefficient by capillarity

43. Lubelli B, RILEM TC 271-ASC (2021) New Accelerated Laboratory Test for the Assessment of the Durability of Materials With Respect To Salt Crystallization. In: Lubelli B, Kamat A, Quist W (eds) SWBSS2021 - Fifth International Conference on Salt Weathering of Buildings and Stone Sculptures. TU Delft Open, pp 55–67

44. Nunes C, Maria Aguilar Sanchez A, Godts S et al (2021) Experimental research on salt contamination procedures and methods for assessment of the salt distribution. Constr Build Mater 298:123862. https://doi.org/10.1016/j.conbuildmat.2021.123862